

Electronic supplementary information

Porous structure and water state in macroporous cross-linked polymer and protein hydrogels produced by cryogelation

Irina N. Savina^{a*}, Vladimir M. Gun'ko^{a,b}, Vladimir V. Turov^b, Maria Dainiak^c,
^s Gary J. Phillips^a, Igor Yu. Galaev^d and Sergey V. Mikhalovsky^a

Received (in XXX, XXX) Xth XXXXXXXXX 200X, Accepted Xth XXXXXXXXX 200X

First published on the web Xth XXXXXXXXX 200X

DOI: 10.1039/b000000x

10

Experimental

Characterisation methods

The hydrogel samples for SEM analysis were prepared by freeze-drying overnight. After drying, specimens were mounted on aluminium stubs fitted with adhesive carbon pads, sputter coated with palladium and examined using a JEOL JSM-6310. Cryo-imaging (cryo-SEM) was carried out using the SEM coupled to a LT400 cryo-unit. A wet hydrogel was mounted onto a cryo-SEM holder and flash frozen in slushy nitrogen. The sample was transferred to the LT400 cryo-unit cooled to -175°C and freeze-fractured to produce a freshly cut surface. The frozen water was sublimed off at -65°C for 30 min, and the sample was sputter-coated with palladium.

Hydrogel samples were examined by confocal laser scanning microscopy with a Leica TCS SP5 CLSM using a regular $20\times$ objective. A slice of approximately 1 mm in thickness was cut from the wet gel and stained with FITC solution (0.02 mg/ml in sodium phosphate buffer, pH 9.0) for 48 h (HEMA-AGE gels) or 20 h (gelatine and gelatine-fibronectin gels). The samples were washed out with buffer and water to remove non-bound FITC. The excitation and emission wavelengths used were 488 and 530 nm, respectively. Images were generated by optical sectioning in the xy-planes along the z-axis with 50 optical sections with 1 μm intervals.

Multiphoton microscopy (MPM) with a Zeiss LSM520 Meta NLO microscope with a Coherent Chameleon XR Ti Sapphire pulsed laser at 800 nm and a water $20\times$ objective was used to study initial hydrogels. Each sample was stained with FITC and prepared as for the CLSM study. MPM scanning was carried out in the z-axis for 87 μm in depth with an image resolution 440 \times 440 pixel. The image resolution depends on the laser beam penetration; therefore, only stacks of 47 images were used to analyse the hydrogel structure.¹

ImageJ² and Fiji³ software was used to determine the structural characteristics of hydrogels. The porosity in the resulting image stack (50 images) was calculated using a Voxel counter plugin.² The calculations were carried out for 2-D images in the stack and average results are obtained.

The surface area and pore interconnectivity was estimated using a 3-D objects counter plugin.^{2,4}

Hydrated fragments (up to 6000 atoms) of polymer and protein hydrogels were calculated using the PM6 method (MOPAC 2009)⁵ with the geometry optimisation using a localised molecular orbital method (MOZYME). The initial structure of the polymer model systems was optimised using the CharMM forcefield (Vega ZZ 2.4.0).⁶ Initial structures of proteins (collagen used instead of gelatine, fibronectin) were taken from the Protein Data Bank.⁷

Differential scanning calorimetry, DSC (Mettler Toledo) measurements were carried out using both hydrated and dried gel samples. The DSC data relating to the melting of frozen water confined in hydrogels as a function of temperature at a certain heating rate were used to determine the size of water clusters, nano- and microdomains bound to/in the gel pore walls.⁸ Water or other liquids can be frozen in narrower pores at lower temperatures that can be described by the Gibbs-Thomson relation for the freezing point depression for cylindrical pore of radius R_p ⁸

$$R_p(\text{nm}) = 0.68 - \frac{32.33}{T_m - T_{m0}}, \quad (\text{S1})$$

where T_m and T_{m0} are the melting temperatures of confined and bulk water, respectively. The pore size distribution (PSD) dV/dR can be calculated from the DSC melting thermograms⁸

$$\frac{dV}{dR}(\text{cm}^3\text{nm}^{-1}\text{g}^{-1}) = \frac{\frac{dq}{dt}(T_m - T_{m0})^2}{32.33\rho\beta m\Delta H(T)}, \quad (\text{S2})$$

where dq/dt , ρ , β , m and $\Delta H(T)$ are the DSC heat flow, the water density, the heating rate, the sample mass and the melting enthalpy of water, respectively. The ΔH values as a function of temperature can be estimated as follows⁸

$$\Delta H(T)(\text{J g}^{-1}) = 332 + 11.39(T_m - T_{m0}) + 0.155(T_m - T_{m0})^2, \quad (\text{S3})$$

The ^1H NMR spectra were recorded at 200–280 K using a Varian 400 Mercury spectrometer of high resolution with 90° probe pulses with the duration of 2 μs . Relative mean errors were $\pm 10\%$ for ^1H NMR signal intensity and $\pm 1\text{ K}$ for temperature. To prevent supercooling of the G gel studied, the temperature dependences of concentration of unfrozen water were determined on the heating of samples pre-cooled to 200 K. The signals of water molecules from ice did not

contribute to the ^1H NMR spectra recorded here because of features of the measurement technique.⁹ Before the measurements, samples (placed in closed NMR ampoules) were equilibrated for 15 min. Changes in the Gibbs free energy (ΔG) of bound water and free surface energy (γ_s), as the modulus of integrated changes of the ΔG values in the bound water layers, were determined from the temperature dependences of the amounts of unfrozen water (C_{uw} in mg of water per gram of dry gelatine gel) at $T = 200\text{--}273\text{ K}$.⁹ Before the NMR measurements, samples were wetted by the addition of a certain amount of water ($h = 0.1$ or 1 g per gram of dried gel) and equilibrated. Several solvents (acetonitrile, chloroform, benzene, Aldrich) miscible or immiscible with water were used in the deuterated form to avoid their contribution to the ^1H NMR signal of adsorbed water unfrozen at $T < 273\text{ K}$. An equation similar to Eq. (S3) was used to estimate the pore size distribution with NMR cryoporometry as described in detail elsewhere.⁹

Results

On image analysis of CLSM and MPM images, a manual “by eye” approach for choosing a proper threshold² was used. However, as a result of image threshold selection (Fig. S1) from 0·4 to 0·20 of grayscale the porosity of HEMA-AGE gel was in the range of 83.0 to 94.6%, the mean pore size increases from 56 to 70 μm and the mean wall thickness reduces from 13 to 9 μm (Table S1). As a whole the results obtained on image analysis can have deviations of $\pm 5\text{--}10\%$ because of the subjective nature of this analysis.

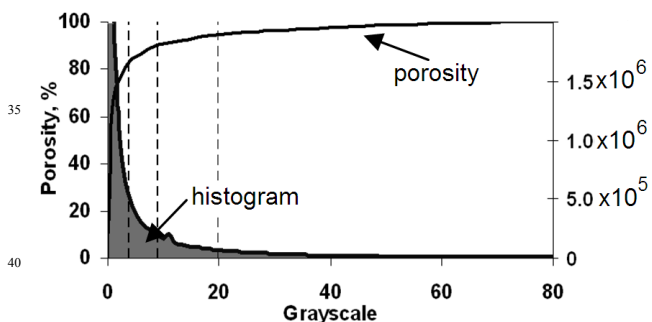


Fig. S1. Effect of threshold selection on porosity estimation for HEMA-AGE hydrogel (sample A); porosity is upper curve (see Table S1).

Additionally, the wall thickness calculated using the granulation plugin² could be overestimated because the software does not distinguish the thickness of walls positioned perpendicular or parallel to the 2-D image plane.

The analysis of HEMA-AGE gels of a varied morphology examined with CLSM (Fig. S2) shows a distinguishable difference in their structure due to different polymerisation conditions.

Soft hydrogels produced using the cryogelation technique can display a different morphology in different layers. The gels produced in the form of cylinders have a

uniform distribution along the sample. Three different regions (cross-sections) in the GF gel were analysed using CLSM.

Table S1. Threshold selection effect on quantification results (HEMA-AGE gel, sample A)

Grayscale range, threshold	0·4	0·9	0·20
Porosity, %	83	90.4	94.6
Mean pore size, d , μm	55.8 ± 8.2	64.0 ± 2.0	69.6 ± 5.6
Mean wall thickness, t , μm	13.3 ± 2.1	11.2 ± 0.83	8.9 ± 2.3

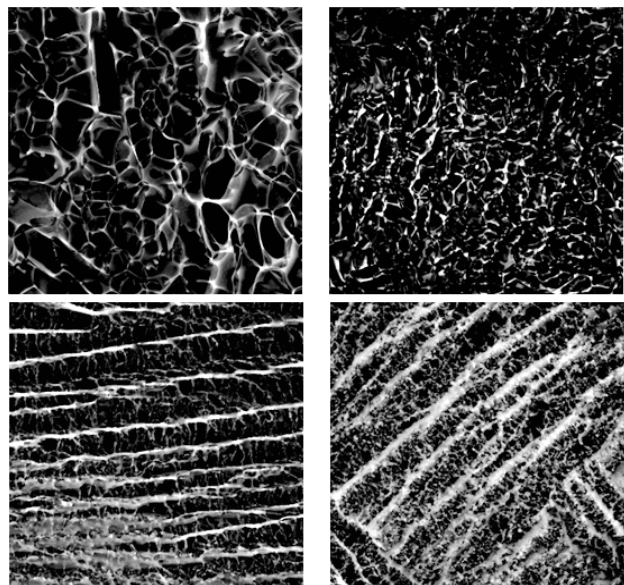


Fig. S2. CLSM images of samples A, B, C and D (Table 1).

The pore size and wall thickness distributions were similar for all the areas analysed. The average porosity, surface area, mean pore size and wall thickness were $87.4 \pm 2.5\%$, $0.049 \mu\text{m}^2/\mu\text{m}^3$, $98 \pm 8.5 \mu\text{m}$ and $18.7 \pm 2.8 \mu\text{m}$, respectively. However, when a gelatine hydrogel is produced as a sheet it has different porosity with large pores at the top layer (in contact with air on the gel preparation) and small pores at the bottom layer (in contact with a glass substrate) (Fig. S3). The pore size, d in this G gel gradually decreased from 76 μm at the sheet top (Fig. S3b), through 54 μm in the middle (Fig. S3c) and 30 μm at the bottom (Fig. S3d). The different porosity in different parts of the hydrogel sample is due to different regimes of heat exchange and hence freezing of the solution in the bulk and at the interfaces liquid-air and liquid-glass. The solution at the glass interface freezes quicker with the formation of small ice crystals, while the solution at the liquid-air interface freezes over a longer period of time resulting in the formation of larger ice crystals. Notice that the G cryogel structure (Fig. S3) differs from the gelatine gel prepared at $T > 0^\circ\text{C}$ ¹⁰ because the cryogelation results in a less uniform and more macroporous structure.

Acknowledgements

This work was financially supported by FP7, projects MACRO-CLEAN (PIEF-GA-2008-220212) and MONACO-EXTRA (PIAP-GA-2008-218242), and the STCU (grant no. 3832, V.V.G. and V.V.T.). Dr. R. Phillips (Sussex University,

UK) is acknowledged for helping with multiphoton microscopy. Mr. M. Helias is acknowledged for helping with

SEM and cryo-SEM.

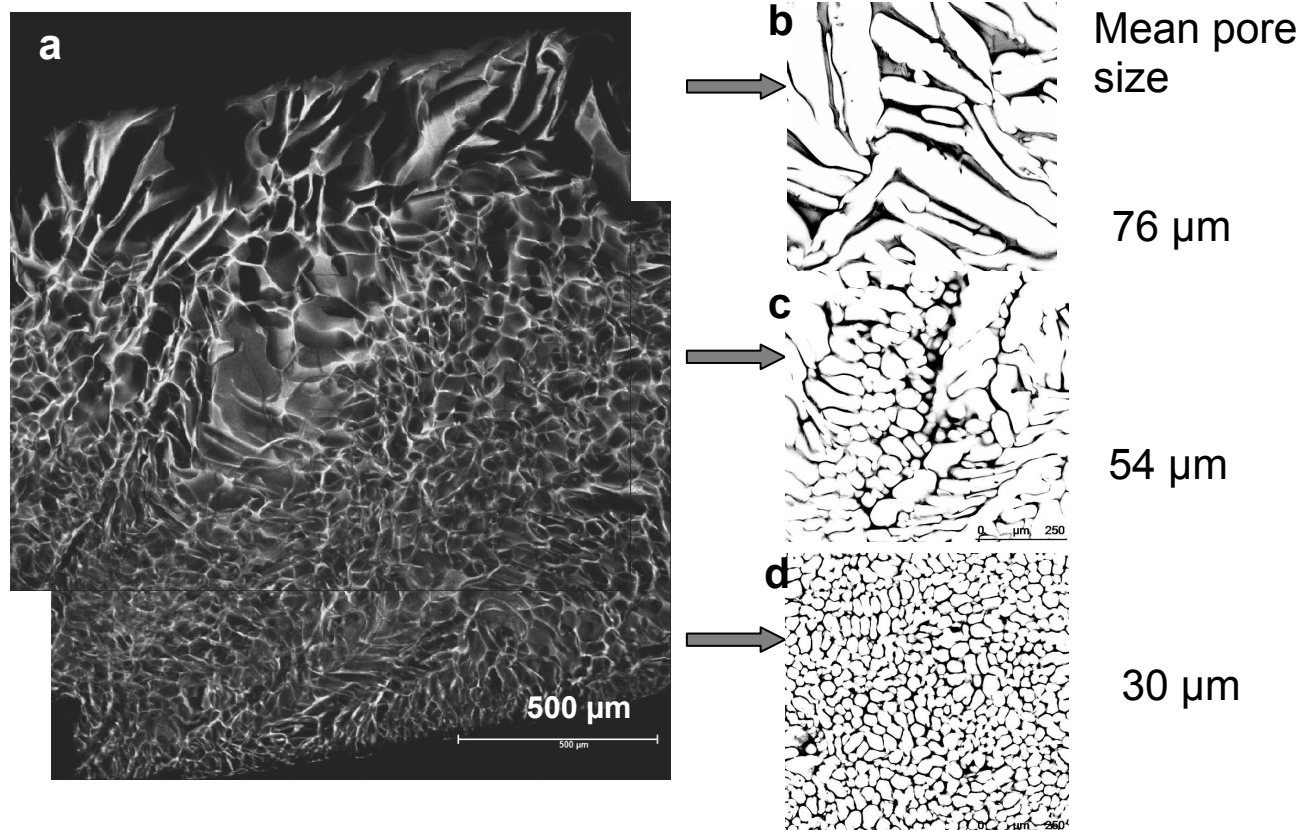


Fig. S3. CLSM image of gelatine sheet cross-section (a); and pore structure of hydrogel for the (b) top, (c) middle and (d) bottom layers.

Notes and references

- ^a University of Brighton, Brighton BN2 4GJ, UK. E-mail: i.n.savina@brighton.ac.uk
10 *Tel: +441273 642015; E-mail: v.gunko@brighton.ac.uk; s.mikhailovsky@brighton.ac.uk;
^b Chuiko Institute of Surface Chemistry, 17 General Naumov Str., Kiev, Ukraine. Fax: +38044 4243567; Tel: 38044 4229627; E-mail: vlad_gunko@ukr.net; v_turov@ukr.net
15 ^c Protista Biotechnology AB, P.O. Box 86, SE-26722 Lund, Sweden. Tel.: +46 286 38 82; fax: +46 286 38 89.
E-mail address: maria.dainiak@protista.se
^d DSM Food Specialties B.V., PO Box 1, 2600 MA Delft, The Netherlands. Tel.: +31 152793771; fax: +31 152794110.
20 E-mail address: igor.galaev@dsm.com

References

- 1 P. Dubrule, R. Unger, S. Van Vlierberghe, V. Cnudde, P. J. S. Jacobs, E. Schacht and C.J. Kirkpatrick, *Biomacromolecules*, 2007, **8**, 338-344. E.L. Hedberg, C.K. Shih, J.J. Lemoine, M.D. Timmer, M.A. Liebschner, J. A. Jansen and A.G. Mikos, *Biomaterials*, 2005, **26**, 3215-3225. I.N. Savina, V. Cnudde, S. D'Hollander, L. Van Hoorebeke, B. Mattiasson, I.Y. Galaev and F. Du Prez, *Soft Matter* 2007, **3**, 1176 - 1184. I.N. Savina, M. Dainiak, H. Jungvid, S.V. Mikhailovsky and I.Y. Galaev, *J. Biomater. Sci.*, 2009, **20**, 1781-1795. F.M. Plieva, J. Andersson, I.Y. Galaev and B. Mattiasson, *J. Sep. Sci.*, 2004, **27**, 828-836.
25 2 <http://rsbweb.nih.gov/ij/download.html>, accessed July 2007. W. Rasband, <http://rsb.info.nih.gov/ij/plugins/voxel-counter.html>,
- 35 accessed July 2007. D. Prodanov, <http://rsb.info.nih.gov/ij/plugins/granulometry.html>, accessed August 2007.
- 3 http://pacific.mpi-cbg.de/wiki/index.php/Main_Page.
- 4 F. Cordelieres, <http://rsb.info.nih.gov/ij/plugins/track/objects.html>, accessed July 2007.
- 40 5 J.P. Stewart, MOPAC2009, Stewart Computational Chemistry, Colorado Springs, CO, USA, <http://openmopac.net/>, 2008.
- 6 A. Pedretti, L. Villa and G. Vistoli, *J. Computer-Aided Mol. Design*, 2004, **18**, 167-173. <http://www.vegazz.net>.
- 7 Protein Data Bank, <http://www.rcsb.org/pdb/>.
- 45 8 M. Chaplin, *Water structure and behavior*. Available from: <<http://www.lsbu.ac.uk/water/>>. M. Brun, A. Lallemand, J.F. Quinson and C. Eyraud, *Thermochim. Acta*, 1977, **21**, 59. J.F. Quinson, N. Mameri, N. Guihard and B. Bariou, *J. Membr. Sci.*, 1991, **58**, 191. J.N. Hay and P.R. Laity, *Polymer*, 2000, **41**, 6171. J.-M. Nedelec and M. Baba, *Recent Res. Devel. Physical Chem.*, 2004, **7**, 381. M.R. Landry, *Thermochim. Acta*, 2005, **433**, 27. J. Weber and L. Bergström, *Langmuir*, 2010, **26**, 10158-10164. G. Rohman, F. Lauprêtre, S. Boileau, P. Guérin and D. Grande, *Polymer*, 2007, **48**, 7017-7028.
- 50 9 V.M. Gun'ko, V.V. Turov, V.M. Bogatyrev, V.I. Zarko, R. Leboda, E.V. Goncharuk, A.A. Novza, A.V. Turov and A.A. Chuiko, *Adv. Colloid Interface Sci.*, 2005, **118**, 25-172.
- 10 10 M. Djabourov, N. Bonnet, H. Kaplan, N. Favard, P. Favard, J. P. Lechaire and M. Maillard, *J. Phys. II France*, 1993, **3**, 611-624.